NASA Technical Memorandum 100277

High Rayleigh Number Convection in Rectangular Enclosures With Differentially Heated Vertical Walls and Aspect Ratios Between Zero and Unity

Siavash A. Kassemi
Lewis Research Center
Cleveland, Ohio

April 1988

NASA

HIGH RAYLEIGH NUMBER CONVECTION IN RECTANGULAR ENCLOSURES WITH DIFFERENTIALLY HEATED VERTICAL WALLS AND ASPECT RATIOS BETWEEN ZERO AND UNITY

Siavash A. Kassemi
National Aeronautics and Space Administration
Lewis Research Center
Cleveland, Ohio 44135

E-3838

SUMMARY

High Rayleigh number convection in a rectangular cavity with insulated horizontal surfaces and differentially heated vertical walls has been analyzed for an arbitrary aspect ratio smaller than or equal to unity. Unlike previous analytical studies, a systematic method of solution based on linearization technique and analytical iteration procedure has been developed to obtain approximate closed-form solutions for a wide range of aspect ratios. The predicted velocity and temperature fields are shown to be in excellent agreement with available experimental and numerical data.

INTRODUCTION

It has long been recognized that the growth of crystals is affected by the fluid dynamics and heat transport characteristics of the process. The flow caused by natural convection has profound influence on the interface shape, defect density, and crystal integrity. As pointed out by Ostrach (ref. 1), high Rayleigh number natural convection flows could still exist under typical conditions in a reduced gravity environment, thereby influencing the growth of crystals. It is, therefore, important to understand the detailed mechanism of convection and flow behavior in order to produce high quality crystals in both ground- and space-based systems.

A configuration containing all the essential physics describing the general flow behavior and transport processes related to crystal growth techniques is that of a rectangular enclosure heated from the side (ref. 2). It is important to note that a central problem inherent to all confined convection situations is that the outer (core) flow region can not be predicted a priori and depends on the boundary layer which, in turn, is influenced by the core (ref. 3). This coupling of the boundary layer and the core region constitutes the main source of difficulty in studying the flow behavior. This matter is not merely a subtlety for analysis but has equal significance for numerical and experimental studies. Because of the complex nature of the problem, numerical and experimental studies must be performed with a high degree of accuracy. Often a prior knowledge of flow behavior such as the extent of boundary layers or location of secondary cells can improve the numerical and experimental studies by allowing the choice of proper mesh sizes and finer measurement techniques. It is therefore apparent that an analytical treatment of this problem, in particular for high Rayleigh number cases where the boundary layers develop, is of considerable importance. Such a treatment (especially if a closed-form solution can be obtained) could greatly enhance the understanding and predict the underlying physics of the problem. However, as stated by Ostrach (ref. 3), most available analytical studies contain unrealistic assumptions and estimates regarding the core configuration which result in solutions

with limited or undefined validity. Moreover, because of special assumptions used in analyzing each particular problem, there seems to be a lack of cohesiveness and systematic approach in treating this type of problem.

Tichy (ref. 4) presents a brief summary of recent work done on high Rayleigh number convection in low aspect ratio cavities. He, himself, obtained analytical-numerical solutions for the low aspect ratio enclosures. Unlike most of the previous analytical studies which concentrate on the prediction of an average Nusselt number, Tichy's work deals with the considerably more complex task of determining the detailed behavior of the flow and temperature fields. He assumes nearly parallel core flow with an aspect ratio $\varepsilon << 1$. His predicted velocities agree reasonably well near centerline regions. In regions away from the centerline, the velocities become less accurate and the no-slip condition on vertical walls is no longer satisfied. Results of other recent investigations include velocity field prediction for $\varepsilon = 1$ by Reddy et al. (ref. 5) for which they use a numerical penalty finite element method of calculation, and the recent work by Kamotani et al. (ref. 6) in which experimental data for Nusselt numbers are obtained for a wide range of important parameters.

To the best of the author's knowledge there has not yet been an analytical investigation for high Rayleigh number natural convection flows for an arbitrary aspect ratio ($0 < \varepsilon \leq 1$). Most of the reported work has been done on very low aspect ratio enclosures and only a few of these studies are concerned with prediction of velocity fields. Moreover, as mentioned earlier, these contain many ad hoc assumptions concerning the nature of the core flow, thereby limiting the validity of solutions. It is the purpose of this study to develop an approximate but systematic analytical method of solution predicting the velocity and temperature distributions in a rectangular cavity with arbitrary aspect ratio $0 < \varepsilon \leq 1$ for the boundary layer region where the Rayleigh number $Ra >> 1$.

In the following analysis a combination of a linearizing method and an analytical iteration procedure is used to obtain approximate closed-form solutions to the problem. Analytical iteration is a useful technique which does not appear to have been fully utilized in fluid mechanics problems such as the present one (ref. 7). When iteration is used in conjuction with another approximate procedure such as a linearization performed on the governing equations, it leads to a powerful but straightforward technique for obtaining approximate, often closed-form, solutions to the problem. This report shows that the solutions obtained for this rather complex problem are in excellent agreement with existing experimental and numerical data.

NOMENCLATURE

A $\quad A = \left[\left(1 - e^{-1/2s}\right)^2 + \dfrac{\lambda_1}{4s^2}\right]$

a $\quad a = Gr^{-1/2}$

B $\quad B = \dfrac{1}{2s} + 2e^{-1/2s} - 0.5e^{-1/s} + \dfrac{\lambda_1}{24s^3}$

b $\quad b = Pr^{-1}$

g acceleration due to gravity

Gr Grashof number, $Gr = \frac{\beta g \, \Delta T H^3}{\nu^2}$

H height of cavity

L width of cavity

ℓ $\quad \ell = -8.31\varepsilon^{-1}Gr^{-1/2}$

M $\quad M(y) = 0.137y + m$

Nu Nusselt number, (eq. (71))

Nu_r Nusselt number referred to in other studies

Pr Prandtl number, $Pr = \frac{\nu}{\alpha}$

Ra Rayleigh number, $Ra = Pr \cdot Gr$

s $\quad s = -\frac{a}{\varepsilon\ell}$

T temperature

T_c temperature of the cold wall

T_h temperature of the hot wall

T_0 $\quad T_0 = \frac{1}{2}(T_h + T_c)$

ΔT $\quad \Delta T = T_h - T_c$

u dimensionless horizontal velocity

v dimensionless vertical velocity

X horizontal coordinate

x dimensionless horizontal coordinate, $x = \frac{X}{L}$

Y vertical coordinate

y dimensionless vertical coordinate, $y = \frac{Y}{H}$

α thermal diffusivity

β $\beta = 41.2m^{7}\varepsilon^{-1}Ra^{-1/4}$

Δ boundary-layer thickness for a vertical plate

δ boundary-layer thickness

ε aspect ratio, $\varepsilon = \frac{H}{L}$

Θ dimensionless temperature, $\Theta = \frac{T - T_o}{\Delta T}$

λ_1 $\lambda_1 = 2s\left(e^{-1/s} - e^{-1/2s}\right)$

μ $\mu = \frac{b^{3/4}Gr^{-1/4}}{8m^3}$

ν kinematic viscosity

Ψ stream function, (eq. (3))

ψ dimensionless stream function, $\psi = \frac{\Psi}{\Psi_R}$

Ψ_R reference stream function, $\Psi_R = \nu Gr^{-1/2}$

Superscripts:

* stretched coordinates

B boundary layer

c core

CB core boundary layer

CC core core

1 first order approximate solutions

2 second order approximate solutions

Subscripts:

t thermal boundary layer thickness

1 unit order variables

MATHEMATICAL FORMULATION

Figure 1 shows a schematic diagram of the physical system. The length of the rectangular cavity is assumed to be much larger than the height and the width so that the problem is two-dimensional. The top and bottom surfaces are thermally insulated and the left and right walls are maintained at isothermal hot and cold temperatures respectively. The flow field is assumed to be steady, laminar, and quasi-incompressible. By quasi-incompressibilty it is meant that the variation in density due to temperature differences are neglected except where they modify the body force term in the momentum equation. This is generally referred to as Boussinesq approximation and has been discussed in a formal way in reference 8.

The stream-function form of governing equations are

$$\nu\psi_R\left[\varepsilon^4\frac{\partial^4\psi}{\partial x^4}+2\varepsilon^2\frac{\partial^4\psi}{\partial x^2\partial y^2}+\frac{\partial^4\psi}{\partial y^4}\right]=-\psi_R^2\,\varepsilon\left[\psi_x\left(\varepsilon^2\psi_{xx}+\psi_{yy}\right)_y-\psi_y\left(\varepsilon^2\psi_{xx}+\psi_{yy}\right)_x\right]+\varepsilon g\beta\,\Delta T H^3\theta_x \tag{1}$$

and

$$\frac{\alpha}{\varepsilon\psi_R}\left(\varepsilon^2\theta_{xx}+\theta_{yy}\right)=-\psi_x\theta_y+\psi_y\theta_x \tag{2}$$

where the stream function is defined by

$$u=\frac{\partial\psi}{\partial y}\qquad v=-\frac{\partial\psi}{\partial x} \tag{3}$$

The pressure term has been eliminated by cross-differentiation of the momentum equations.

The above equations are also nondimensionalized by use of the following variables:

$$x=\frac{X}{L}\qquad y=\frac{Y}{H}\qquad \theta=\frac{T-T_0}{\Delta T}\qquad \psi=\frac{\Psi}{\psi_R}\qquad \varepsilon=\frac{H}{L} \tag{4}$$

Notice that the reference stream function ψ_R is left unspecified and will be determined by a proper force balance as appropriate to the problem. For $Gr \gg 1$, $Pr \sim 1$ the correct force balance is obtained by equating the coefficient of inertia and buoyancy terms in the vorticity equation (refs. 9 and 10). This yields to the proper characteristic stream function given by

$$\psi_R=\nu\sqrt{Gr} \tag{5}$$

By substituting equation (5) into equations (1) and (2) the final form of the system of equations to be solved becomes

$$\frac{\alpha}{\varepsilon}\left(\varepsilon^4\psi_{xxxx} + 2\varepsilon^2\psi_{xxyy} + \psi_{yyyy}\right) = -\psi_x\left(\varepsilon^2\psi_{xxy} + \psi_{yyy}\right) + \psi_y\left(\varepsilon^2\psi_{xxx} + \psi_{xyy}\right) + \theta_x \tag{6}$$

$$\frac{ab}{\varepsilon}\left(\varepsilon^2\theta_{xx} + \theta_{yy}\right) = -\psi_x\theta_y + \psi_y\theta_x \tag{7}$$

where

$$a = Gr^{-1/2}$$

and

$$b = Pr^{-1}$$

The boundary conditions are

$$\left.\begin{aligned} &\psi = \psi_x = 0 \quad \text{at} \quad x = \pm\frac{1}{2} \\ &\psi = \psi_y = 0 \quad \text{at} \quad y = \pm\frac{1}{2} \\ &\theta = \pm\frac{1}{2} \quad \text{at} \quad x = \pm\frac{1}{2} \\ &\theta_y = 0 \quad \text{at} \quad y = \pm\frac{1}{2} \end{aligned}\right\} \tag{8}$$

NORMALIZED BOUNDARY LAYER EQUATIONS

The normalized boundary-layer equations are derived by properly balancing forces within the regions where they act. For Prandtl numbers larger than or equal to unity, the thermal boundary-layer thickness is smaller than, or at most equal to, the momentum boundary-layer thickness. In this case viscous and bouyant forces can then be assumed to be of the same order of magnitude within the thermal boundary-layer region (refs. 11 and 12). Stretching the coordinate normal to the vertical wall and expanding $\overset{B}{\psi}$ and $\overset{B}{\theta}$ in asymptotic series (ref. 9) gives

$$\overset{*}{x} = \frac{x + \frac{1}{2}}{\delta_t} \tag{9}$$

$$\overset{B}{\psi} = E_1\overset{B}{\psi_1} + \ldots \tag{10}$$

$$\overset{B}{\theta} = \overset{B}{\theta_1} + \ldots \tag{11}$$

Substituting into general equations (6) and (7) and equating the coefficients of convective and conductive terms as well as viscous and buoyancy terms determine the unknown parameters δ_t and E_1

$$\delta_t = \varepsilon Ra^{-1/4} = \varepsilon b^{1/4} a^{1/2} \tag{12}$$

$$E_1 = Pr^{-3/4} Gr^{-1/4} = b^{3/4} a^{1/2} \tag{13}$$

and the boundary-layer equations given by

$$\overset{B}{\psi}_{1_{xxxx}}^{****} = -b\left[\overset{B}{\psi}_{1_x}^{*}\overset{B}{\psi}_{1_{xxy}}^{**} - \overset{B}{\psi}_{1_y}\overset{B}{\psi}_{1_{xxx}}^{***}\right] + \overset{B}{\theta}_{1_x}^{*} \tag{14}$$

and

$$\overset{B}{\theta}_{1_{xx}}^{**} = -\overset{B}{\psi}_{1_x}^{*}\overset{B}{\theta}_{1_y} + \overset{B}{\psi}_{1_y}\overset{B}{\theta}_{1_x}^{*} \tag{15}$$

The outer flow region or core equations are obtained by letting $a \to 0$ in equations (6) and (7). This gives

$$\overset{C}{\psi}_x\left(\varepsilon^2\overset{C}{\psi}_{xxy} + \overset{C}{\psi}_{yyy}\right) - \overset{C}{\psi}_y\left(\varepsilon^2\overset{C}{\psi}_{xxx} + \overset{C}{\psi}_{xyy}\right) = \overset{C}{\theta}_x \tag{16}$$

$$\overset{C}{\psi}_x\overset{C}{\theta}_y - \overset{C}{\psi}_y\overset{C}{\theta}_x = 0 \tag{17}$$

The system of equations (6) and (7) has now been broken into the boundary-layer and core equations (14) to (17). An analytical iterative technique is used to find approximate solutions which satisfy equations (14) to (17). It is important to note that in an iterative process the accuracy of the solution depends on the number of iterations; therefore, if a limited number of iterations are desired, the choice of the initial profiles becomes very important. Consequently, if the initial profile is chosen so that it is most compatible with the particular assumptions and physics of the problem then the resulting solution will be satisfactory after only a few iterations. In the present problem the highest temperature changes occur within the thermal boundary-layer region near the vertical walls. Therefore the buoyant forces are very strong within that region, whereas in the core region the bouyant forces are weak because of the absence of sharp temperature gradients. Since the buoyancy is the main driving force here, it is important to choose an initial profile such that the change of buoyancy in the x-direction is accounted for. Accordingly we let

$$\overset{1}{\psi} = C_1(x)(16y^4 - 8y^2 + 1) \tag{18}$$

$$\overset{1}{\theta} = D_0(x) + D_1(x)(4y^3 - 3y) \tag{19}$$

These profiles satisfy the horizontal wall conditions at $y = \pm 1/2$. Substituting equations (18) and (19) into equations (14) to (17) yields the following equations:

$$b^{-3/4}Gr^{1/4}{}^{B''''}_{C_1}(16y^4 - 8y^2 + 1) = b^{-1/2}Gr^{1/2}\left\{-\left[{}^{B'}_{C_1}(16y^4 - 8y^2 + 1)\right]\right.$$

$$\left.\left[{}^{B''}_{16C_1}(4y^3 - y)\right] + \left[{}^{B}_{16C_1}(4y^3 - y)\right]\left[{}^{B'''}_{C_1}(16y^4 - 8y^2 + 1)\right]\right\} + {}^{B'}_{D_0} + {}^{B'}_{D_1}(4y^3 - 3y) \tag{20}$$

$${}^{B''}_{D_0} + {}^{B''}_{D_1}(4y^3 - 3y) = b^{-3/4}Gr^{1/4}\left\{-\left[{}^{B'}_{C_1}(16y^4 - 8y^2 + 1)\right]\left[{}^{B}_{3D_1}(4y^2 - 1)\right]\right.$$

$$\left. + \left[{}^{B}_{16C_1}(4y^3 - y)\right]\left[{}^{B'}_{D_0} + {}^{B'}_{D_1}(4y^3 - 3y)\right]\right\} \tag{21}$$

and

$$\left[{}^{C'}_{C_1}(16y^4 - 8y^2 + 1)\right]\left[16\varepsilon^2{}^{C''}_{C_1}(4y^3 - y) + {}^{C}_{384C_1}y\right] - \left[{}^{C}_{16C_1}(4y^3 - y)\right]$$

$$\left[{}^{C'''}_{C_1}(16y^4 - 8y^2 + 1) + {}^{C'}_{16C_1}(12y^2 - 1)\right] = {}^{C'}_{D_0} + {}^{C'}_{D_1}(4y^3 - 3y) \tag{22}$$

$$\left[{}^{C'}_{C_1}(16y^4 - 8y^2 + 1)\right]\left[{}^{C}_{3D_1}(4y^2 - 1)\right] = \left[{}^{C}_{16C_1}(4y^3 - y)\right]\left[{}^{C'}_{D_0} + {}^{C'}_{D_1}(4y^3 - 3y)\right] \tag{23}$$

Note, that based on the discussion presented above, the functions $C_1(x)$, $D_0(x)$, and $D_1(x)$ have been broken into boundary-layer and core contributions, thus accounting for varied buoyant action in the x-direction. Assuming the existence of an overlap region wherein both the core and the boundary-layer expansions remain valid, the following matching conditions must hold (see ref. 9):

$$\lim_{X\to\infty}{}^{1B}_{\theta_*} = {}^{1C}_{\theta_X} \to -1/2$$

$$\lim_{X\to\infty}{}^{1B}_{\psi_*} = {}^{1C}_{\psi_X} \to -1/2$$

$$\left.{}^{1B}_{\psi_{*_X}}\right|_{X\to\infty} = \left.{}^{1C}_{\psi_X}\right| x \to -1/2 \tag{24}$$

In order to solve the nonlinear and coupled boundary-layer and core equations (eqs. (20) to (23)), the following boundary-layer profiles, which satisfy the left wall conditions, are assumed:

$$C_1^B = Mb^{3/4}Gr^{-1/4}\left[1 + \left(\sin m\overset{*}{x} - \cos m\overset{*}{x}\right)e^{m\overset{*}{x}}\right] \tag{25}$$

$$D_0^B = \frac{1}{2}\cos m\overset{*}{x}e^{m\overset{*}{x}} \tag{26}$$

$$D_1^B = L\left(1 - \cos m\overset{*}{x}e^{m\overset{*}{x}}\right) \tag{27}$$

An identical procedure can be used for the right wall.

The above functional forms are systematically predicted by utilizing the wall conditions, along with a linearized solution to the nonlinear equations. (See ref. 9 for a detailed description of "the modified Oseen linearization technique.") The unknown constants are determined by requiring the assumed profiles (18) and (19) to satisfy the integral form of governing equations in the y-direction and across the vertical boundary layer. The core region in the x-direction satisfies the core equations (16) and (17) exactly. The core and boundary-layer stream function and temperature are then

$$\psi^{1B} = \frac{b^{3/4}Gr^{-1/4}}{8m^3}\left[1 + \left(\sin m\overset{*}{x} - \cos m\overset{*}{x}\right)e^{m\overset{*}{x}}\right](4y^2 - 1)^2 \tag{28}$$

$$\theta^{1B} = \frac{1}{2}e^{m\overset{*}{x}} - 1.78m^4\left(1 - \cos m\overset{*}{x}e^{m\overset{*}{x}}\right)(4y^3 - 3y) \tag{29}$$

$$\psi^{1C} = \frac{b^{3/4}Gr^{-1/4}}{8m^3}(4y^2 - 1)^2 \tag{30}$$

$$\theta^{1C} = -1.78m^4(4y^3 - 3y) \tag{31}$$

where m is an unknown constant to be determined later. The total stream function and temperature can be constructed by using the composition rule (ref. 13). We then obtain

$$\psi^{1} = \frac{b^{3/4}Gr^{-1/4}}{8m^3}\left[1 + \left(\sin m\overset{*}{x} - \cos m\overset{*}{x}\right)e^{m\overset{*}{x}}\right](4y^2 - 1)^2 \tag{32}$$

$$\theta^{1} = \frac{1}{2}e^{m\overset{*}{x}} - 1.78\ m^4\left(1 - \cos m\overset{*}{x}e^{m\overset{*}{x}}\right)(4y^3 - 3y) \tag{33}$$

To estimate m, the boundary-layer equation (14) is integrated from $\overset{*}{x} = 0$ to $\overset{*}{x} = \Delta/\delta$ at $y = 0$. The boundary-layer thickness Δ at $y = 0$ is taken to be the same as the boundary-layer thickness on a flat plate at that location, (ref. 14); this yields

$$m = -0.56 \tag{34}$$

Equations (28) to (33) are approximate solutions satisfying the boundary conditions on the walls and the integral form of governing equations. Although it is not shown here (for brevity), the above solutions predict the average Nusselt number and temperature field in good agreement with numerical and experimental data. Because of the averaged nature of the first approximation, however, the velocity fields are only in qualitative agreement with experimental and numerical data. Therefore it seems reasonable that a refinement of solutions through an analytical iterative process should yield solutions in full agreement with existing studies. This is indeed the case as will be seen by comparing the iterated solutions to available data. (See section Results and Discussion.)

By proceeding in the same manner as explained in reference 7, the approximate results obtained for the core stream function and temperature (eqs. (30) and (31)) are utilized in the original vorticity equation to obtain a more accurate core solution. The core variables $\overset{1C}{\psi}$ and $\overset{1C}{\theta}$ obtained previously are a function of y only. Therefore, the new core variables $\overset{2C}{\psi}$ and $\overset{2C}{\theta}$ can be expected to deviate only by a small margin from $\overset{1C}{\psi}$ and $\overset{1C}{\theta}$. Hence the new variables must satisfy the condition

$$\frac{\partial \overset{2C}{\psi}}{\partial x} << \frac{\partial \overset{2C}{\psi}}{\partial y} \quad \text{and} \quad \frac{\partial \overset{2C}{\theta}}{\partial x} << \frac{\partial \overset{2C}{\theta}}{\partial y} \tag{35}$$

Using condition (35) in the original vorticity equation (6) results in the general core vorticity equation

$$\frac{a}{\varepsilon} \overset{2C}{\Psi}_{yyyy} + \overset{2C}{\Psi}_x \overset{2C}{\Psi}_{yyy} - \overset{2C}{\Psi}_y \overset{2C}{\Psi}_{xyy} = \overset{2C}{\Theta}_x \tag{36}$$

The core temperature obtained in the first approximation is now substituted in the right-hand side of equation (36) to yield

$$\frac{a}{\varepsilon} \overset{2C}{\Psi}_{yyyy} + \overset{2C}{\Psi}_x \overset{2C}{\Psi}_{yyy} - \overset{2C}{\Psi}_y \overset{2C}{\Psi}_{xyy} = 0 \tag{37}$$

Assuming $\overset{2C}{\psi} = X(x)Y(y)$, we obtain

$$X' = \ell \tag{38}$$

and

$$aY'''' + \varepsilon\ell(YY''' - Y'Y'') = 0 \tag{39}$$

Note that equation (39) has boundary-layer characteristics (i.e., as $a \to 0$ the highest derivative term vanishes); hence all boundary conditions on horizontal walls cannot be satisfied. Equation (39) can therefore be broken up into core and boundary-layer equations

$$\overset{CC}{Y}\overset{CC}{Y}'' - \overset{CC}{Y}'\overset{CC}{Y}'' = 0 \tag{40}$$

and

$$\frac{d^4 Y^{CB}}{d\overset{*}{y}^4} + Y^{CB}\frac{dY^{3CB}}{d\overset{*}{y}^3} - \frac{dY^{CB}}{d\overset{*}{y}}\frac{dY^{2CB}}{d\overset{*}{y}^2} = 0 \tag{41}$$

where $\overset{*}{y}$ is the usual stretched coordinate

$$\overset{*}{y} = \frac{\frac{1}{2} - y}{s} \qquad \text{for} \quad y \geqq 0 \tag{42}$$

and superscripts "CB" and "CC" refer to "core boundary layer" and "core core" respectively. The parameter s is defined

$$s = -\frac{a}{\varepsilon \ell} \tag{43}$$

Omitting the details, it can be shown that equation (40) has an approximate solution which is

$$y^{CC} \cong A_1 y^2 + A_2 y + A_3 \tag{44}$$

The solution to the core boundary-layer equation (41) can be obtained by using an integral method, which is customary for finding approximate solutions to boundary-layer equations. A suitable profile that satisfies the horizontal wall conditions is given by

$$y^{CB} = C\left(1 - e^{-\overset{*}{y}}\right)^2 \tag{45}$$

where C is a constant to be determined later. The profile equation (45) will later be forced to satisfy the integral form of equation (41). For the core stream functions we obtain

$$\psi^{CB} = C(\ell x + 1)\left(1 - e^{-\overset{*}{y}}\right)^2 \tag{46}$$

$$\psi^{CC} = (\ell x + 1)(A_1 y^2 + A_2 y + A_3) \tag{47}$$

Equations (46) and (47) must match at an intermediate region (ref. 13) as follows

$$\psi^{CB}(x,\infty) = \psi^{CC}\left(x, \frac{1}{2}\right) \tag{48}$$

$$\psi_y^{CB}(x,\infty) = \psi_y^{CC}\left(x, \frac{1}{2}\right) \tag{49}$$

The composition rule for stream functions gives

$$\psi^{C} = \psi^{CB} + \psi^{CC} - \psi^{CB}(x,\infty) \tag{50}$$

Therefore the total core stream function is

$$\psi^{2C} = C(\ell x + 1)\left[\left(1 - e^{-y^*}\right)^2 + \lambda_1 y^{*2}\right] \tag{51}$$

where λ_1 is a constant to be determined. It is now necessary to satisfy the core boundary-layer equation (41) by ψ^{CB} on an integral basis. In addition, the "centro-symmetry" property (ref. 10) requires that

$$\psi^{2C}_y(0,0) = 0 \tag{52}$$

In the same manner as Collatz (ref. 7), the value of ψ^{2C} at $x = 0$ and $y = 0$ will be set equal to the value of ψ^{1C} at $x = 0$ and $y = 0$. The above constraints are sufficient to determine all constants in equation (51). These are

$$\left.\begin{aligned} \lambda_1 &= 2s\left(e^{-1/s} - e^{-1/2s}\right) \\ &\text{where} \\ s &= 0.12 \\ &\text{and} \\ C = A\mu &= \frac{b^{3/4}Gr^{-1/4}}{8m^3}A \\ &\text{where} \\ A &= \frac{1}{\left[\left(1 - e^{-1/2s}\right)^2 + \lambda_1(1/2s)^2\right]} \end{aligned}\right\} \tag{53}$$

From relation (43), the parameter ℓ is

$$\ell = -\frac{8.31}{\varepsilon Gr^{1/2}} \tag{54}$$

Therefore when $Gr \gg 1$, and $0|x| < 1/2$, ℓx is negligible with respect to unity, and we obtain

$$\psi^{2C} = A\mu\left[\left(1 - e^{-y^*}\right)^2 + \lambda_1 y^{*2}\right] \tag{55}$$

A more accurate boundary-layer velocity can now be obtained by modifying the boundary-layer solution $\overset{1B}{\psi}$ of equation (28) to satisfy the asymptotic matching condition with the new core stream function $\overset{2C}{\psi}$ of equation (55); that is, let

$$\overset{2B}{\psi} = A\mu \left\{1 + \left[\sin\left[(M(y)\overset{*}{x}\right] - \cos\left[M(y)\overset{*}{x}\right]\right] e^{(M(y)\overset{*}{x})}\right\} \left[\left(1 - e^{-\overset{*}{y}}\right)^2 + \lambda_1 \overset{*2}{y}\right] \tag{56}$$

where the parameter M is an unknown function of y to be specified later. Note that the core-boundary-layer velocity matchings are satisfied; that is

$$\overset{2B}{\psi}(\infty, y) = \overset{2C}{\psi}\left(-\frac{1}{2}, y\right) \tag{57}$$

and

$$\overset{2B}{\psi}_{\overset{*}{x}}(\infty, y) = \overset{2C}{\psi}_x\left(-\frac{1}{2}, y\right) \tag{58}$$

Also note that $\overset{2B}{\psi}$ satisfies the horizontal wall conditions. Assuming the simplest linear profile for $M(y)$ and requiring that $\overset{2B}{\psi}$ is satisfied by the integral form of the boundary-layer energy equation (15) yields

$$M(y) = 0.137y + m \tag{59}$$

Again, using the composite rule for determining the total stream function, we obtain

$$\overset{2}{\psi} = A\mu \left\{1 + \left[\sin\left[(0.137y + m)\overset{*}{x}\right] - \cos\left[(0.137y + m)\overset{*}{x}\right]\right] e^{(0.137y + m)\overset{*}{x}}\right\} \left[\left(1 - e^{-\overset{*}{y}}\right)^2 + \lambda_1 \overset{*2}{y}\right] \tag{60}$$

from which the velocities can be derived

$$\overset{2}{v} = A\mu \left\{-\frac{2(0.137y + m)}{\delta_t} \sin\left[(0.137y + m)\overset{*}{x}\right] e^{(0.137y + m)\overset{*}{x}}\right\} \left[\left(1 - e^{-\overset{*}{y}}\right)^2 + \lambda_1 \overset{*2}{y}\right] \tag{61}$$

$$u^2 = -\frac{2A\mu}{s}\left\{1 + \left[\sin\left[(0.137y + m)x^*\right] - \cos\left[(0.137y + m)x^*\right]\right]\right.$$

$$\left. e^{(0.137y + m)x^*}\right\}\left(e^{-y^*} - e^{2y^*} + \lambda_1 y^*\right) + 0.274A\mu\left\{x^* \sin\left[(0.137y + m)x^*\right]\right.$$

$$\left. e^{(0.137y + m)x^*}\right\}\left[\left(1 - e^{-y^*}\right)^2 + \lambda_1 y^{*2}\right] \qquad (62)$$

In a similar manner, a better approximation can be obtained for the core temperature. The new temperature θ^{2C} must satisfy the general core energy equation given by

$$\frac{ab}{\varepsilon}\theta^{2C}_{yy} = \psi^{2C}_y \theta^{2C}_x - \psi^{2C}_x \theta^{2C}_y \qquad (63)$$

Because of horizontal wall conditions imposed on θ^{2C}, it must be of the form

$$\theta^{2C} = g(y) + f(x) \qquad (64)$$

Substituting equation (64) into equation (63) yields

$$\frac{\alpha b}{\varepsilon} g''(y) = f'(x)\left\{A\mu\left[\left(1 - e^{-y^*}\right)^2 + \lambda_1 y^{*2}\right]\right\}' \qquad (65)$$

This necessitates that,

$$f'(x) = \text{const.} = \beta \qquad (66)$$

and hence

$$\frac{ab}{\varepsilon} y'' = \beta A\mu\left[\left(1 - e^{-y^*}\right)^2 + \lambda_1 y^{*2}\right] \qquad (67)$$

Using the horizontal wall condition and employing the central symmetry property $\theta^{2C}(0,0) = 0$ yield

$$\theta^{2C} = \frac{A\mu\beta\varepsilon s}{ab}\left(-y^* - 2e^{-y^*} + \frac{1}{2}e^{-2y^*} - \frac{\lambda_1}{3}y^{*3} + B\right) + \beta x \qquad (68)$$

Guided by the boundary-layer solution for $\overset{1}{\theta}$, we let

$$\overset{2B}{\theta} = \frac{1}{2} e^{m\overset{*}{x}} + \left[1 - \cos(m\overset{*}{x})e^{m\overset{*}{x}}\right]\left[\frac{A\mu\beta\varepsilon s}{ab}\left(-\overset{*}{y} - 2e^{-\overset{*}{y}} + \frac{1}{2} e^{2\overset{*}{y}} - \frac{\lambda_1}{3}\overset{*3}{y} + B\right) - \frac{\beta}{2}\right] \tag{69}$$

where the core-boundary-layer matching conditions are satisfied for $\overset{2}{\theta}$.

By the composition principle, the total temperature is constructed and reads

$$\overset{2}{\theta} = \frac{1}{2} e^{m\overset{*}{x}} + \left[1 - \cos(m\overset{*}{x})e^{m\overset{*}{x}}\right]\left[\frac{A\mu\beta\varepsilon s}{\alpha b}\left(-\overset{*}{y} - 2e^{-2\overset{*}{y}} + \frac{1}{2} e^{-2\overset{*}{y}} - \frac{\lambda_1}{3}\overset{*3}{y} + B\right) - \frac{\beta}{2}\right] + \beta\left(x + \frac{1}{2}\right) \tag{70}$$

Defining the average dimensionless heat transfer coefficient at the wall by

$$Nu = \int_{y=-1/2}^{1/2} \theta_x\Big|_{x=-1/2} dy \tag{71}$$

we then obtain

$$Nu = \frac{m}{2\delta}(1 + \beta) \tag{72}$$

The reference Nusselt number used for comparison purposes can be shown to be related to Nu by

$$Nu_r = \varepsilon Nu \tag{73}$$

and hence

$$Nu_r = \frac{m\varepsilon}{2\delta}(1 + \beta) \tag{74}$$

To obtain an estimate for β, we require that $\overset{2C}{\theta}_y$ and $\overset{1C}{\theta}_y$ be of the same order of magnitude in the $0 \leqq y \leqq 1/2$ range (see ref. 7); that is,

$$\int_{y=0}^{1/2} \overset{2C}{\theta}_y \, dy = \int_{y=0}^{1/2} \overset{1C}{\theta}_y \, dy \tag{75}$$

This gives

$$\beta = \frac{41.2m^7 Ra^{-1/4}}{\varepsilon} \tag{76}$$

With determination of the parameter β, the solution to the problem is complete. The approximate, closed-form solutions derived for the velocity and temperature fields now can be used conveniently to obtain detailed information about the flow behavior and heat transfer characteristics of the problem. In the next section the present solutions are carefully examined and comparisons to existing experimental and numerical data are made.

RESULTS AND DISCUSSION

In order to test the validity and accuracy of the solutions, a number of cases were calculated to enable a comparison with established experimental and numerical results of other investigations.

The vertical and horizontal velocities as given by equations (61) and (62) have been plotted and compared to several existing numerical and experimental data for different values of the aspect ratio.

Figure 2 shows a plot of the end vertical velocity profiles for $Ra = 3 \times 10^8$, $Pr = 1$, $\varepsilon = 0.1$, and $y = \pm 0.179$. The present solution in both the $y = +0.179$ and $y = -0.179$ regions agrees very well with numerical data. The fact that Tichy's analytical solution does not satisfy the no-slip conditions at vertical walls except at $y = 0$ is partially responsible for a less quantitative agreement between his analytical and numerical solutions. Note that in the present study all wall conditions are satisfied.

Figure 3 compares the present analytical solutions of mid-core velocities with Tichy's numerical solutions (ref. 4). The agreement is good for all velocities. It is especially important to note that the horizontal boundary-layer character of the flow for very large values of Rayleigh numbers is evident both in numerical and analytical solutions. Because of the centro-symmetric property, only the top part of velocities are drawn. The Rayleigh number ranges from 10^7 to 10^9 with $Pr = 1$ and $\varepsilon = 0.1$.

In figure 4 the vertical velocity along the centerline of the enclosure is plotted and compared with numerical data of reference 5 which were obtained by using a penalty finite element method. There is good agreement through the entire region. In this case $Ra = 10^5$, $Pr = 1$, and the aspect ratio ε is equal to unity (i.e., a square cavity). This, once again, emphasizes the wide range of applicability of the present solution.

The average wall Nusselt number is plotted in figure 5. At very high Rayleigh numbers, $Ra \sim 10^9$, the average heat transfer coefficient is practically independent of the aspect ratio ε. For moderately high Rayleigh numbers of $Ra < 10^9$ the impact of the aspect ratio ε becomes more obvious however, and results in a splitting of the Nusselt number curves which correspond to low aspect ratio enclosures and enclosures with aspect ratios near unity. The recent experiments by Kamotani, et al. (ref. 6) clearly support the current predictions.

Figure 6 shows plots of the core temperature measured at three different x-locations and for the low aspect ratio of $\varepsilon = 0.0625$ (ref. 6). The solid line is the core temperature distribution derived in the present analysis. There is good agreement between the analytical and experimental temperature fields.

CONCLUSIONS

The problem of high Rayleigh number natural convection for arbitrary aspect ratio, $0 < \varepsilon \leqq 1$, has been solved analytically. A combination of a linearizing method and an analytical iteration technique was used. This combination of techniques ultimately led to closed-form approximate solutions for velocity and temperature fields (eqs. (61), (62), and (70)). There are two major differences between this work and all of the known previous efforts; one is the wide range of applicability for the aspect ratio ($0 < \varepsilon \leqq 1$), and the other is the fact that the method of solution has been systematic, with no a priori assumptions made regarding, for example, the core configurations. This approach is especially important for even more complicated problems such as the study of multispecies natural convection where clear experimental and numerical data are not available for use in theoretical analysis.

REFERENCES

1. Ostrach, S.: Convection Phenomena at Reduced Gravity of Importance for Materials Processing in Space. Materials Sciences in Space With Application to Space Processing, L. Steg, ed., AIAA, 1977, pp. 3-32.

2. Ostrach, S.: Fluid Mechanics in Crystal Growth - The 1982 Freeman Scholar Lecture. J. Fluids Eng., vol. 105, no. 1, Mar. 1983, pp. 5-20.

3. Ostrach, S.: Natural Convection Heat Transfer in Cavities and Cells. Heat Transfer 1982, Vol. I, U. Grigull, et al., eds., Hemisphere Publishing Co., 1982, pp. 365-379.

4. Tichy, J.; and Gadgil, A.: High Rayleigh Number Laminar Convection in Low Aspect Ratio Enclosures with Adiabatic Horizontal Walls and Differentially Heated Vertical Walls. J. Heat Trans., vol. 104, no. 1, Feb. 1982, pp. 103-110.

5. Reddy, J.N.; and Satake, A.: A Comparison of a Penalty Finite Element Model with the Stream Function-Vorticity Model of Natural Convection in Enclosures. J. Heat Trans., vol. 102, no. 4, Nov. 1980, pp. 659-666.

6. Kamotani, Y.; Ostrach, S.; and Wang, L.W.: Experiments on Natural Convection Heat Transfer in Low Aspect Ratio Enclosures. AIAA J., vol. 21, no. 2, Feb. 1983, pp. 290-294.

7. Collatz, L.: The Numerical Treatment of Differential Equations. 3rd edition, Springer-Verlag, 1960.

8. Ostrach, S.: Laminar Flows with Body Forces. Theory of Laminar Flows, High-Speed Aerodynamics and Jet Propulsion, Vol. 4, F.K. Moore, ed., Princeton University Press, Princeton, N.J., 1964, Section D. (NASA TM X-68960).

9. Ostrach, S.; and Hantman, R.G.: Natural Convection Inside A Horizontal Cylinder. Chem. Eng. Commun., vol. 9, nos. 1-6, 1981, pp. 213-243.

10. Kassemi, S.A.: Thermal and Double-Diffusive Natural Convection Inside A Horizontal Cylinder. Ph.D. Thesis, Case Western Reserve University, 1986.

11. Ostrach, S.: Low-Gravity Fluid Flows. Annual Review of Fluid Mechanics, Vol. 14, M. Van Dyke, J.V. Wehausen, and J.L. Lumley, eds., Annual Reviews Inc., Palo Alto, CA, 1982, pp. 313-345.

12. Braun, W.H.; and Heighway, J.E.: An Integral Method for Natural-Convection Flows at High and Low Prandtl Numbers. NASA TND-292, 1960.

13. Van Dyke, M.: Perturbation Methods in Fluid Mechanics. Academic Press, 1964.

14. Elder, J.W.: Laminar Free Convection In A Vertical Slot. J. Fluid Mech., vol. 23, pt 1, Sept. 1965, pp. 77-98.

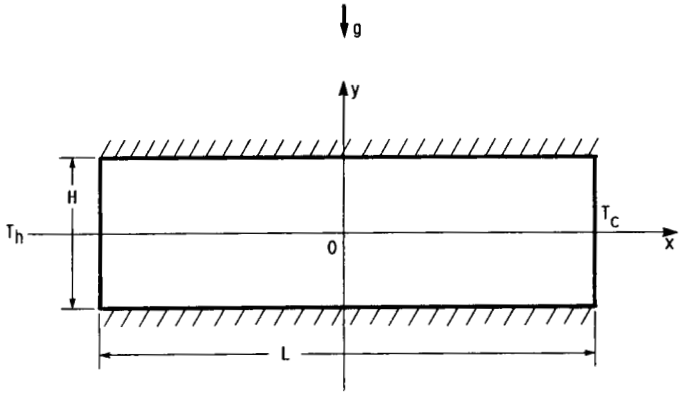

FIGURE 1. - PHYSICAL SYSTEM.

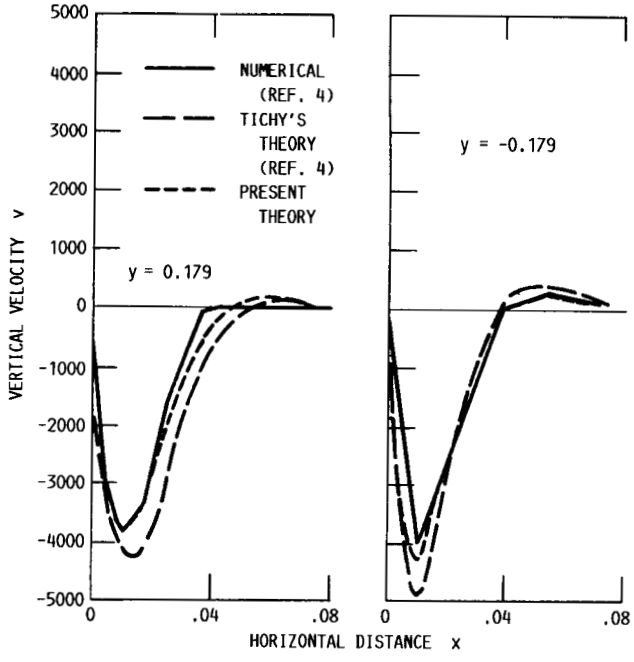

FIGURE 2. - END VERTICAL VELOCITY PROFILES OF ANALYTICAL AND NUMERICAL RESULTS; Ra = 3×10^8, y = ±0.179, ε = 0.1, Pr = 1.

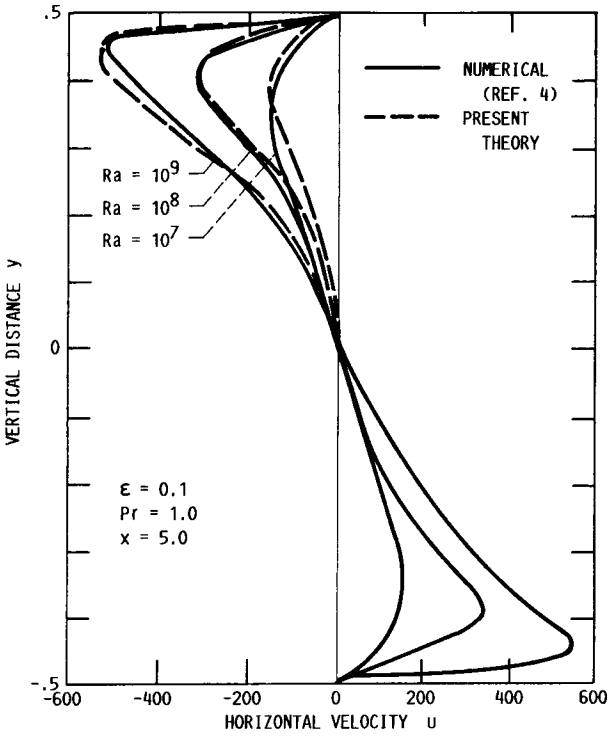

FIGURE 3. - CORE HORIZONTAL VELOCITY PROFILES OF ANALYTICAL AND NUMERICAL RESULTS.

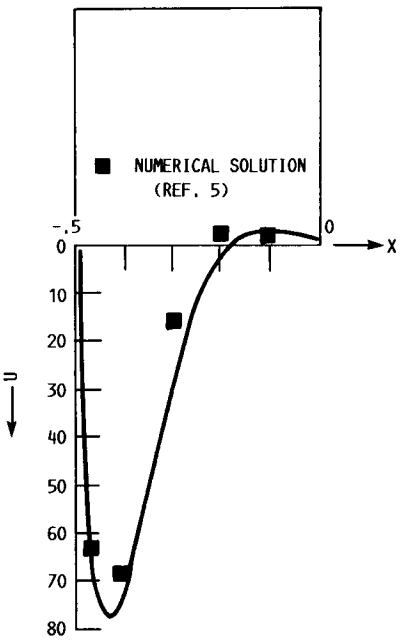

FIGURE 4. - VELOCITY DISTRIBUTION ALONG THE CENTER LINE OF THE ENCLOSURE; Pr = 1, Ra = 10^5, ε = 1.

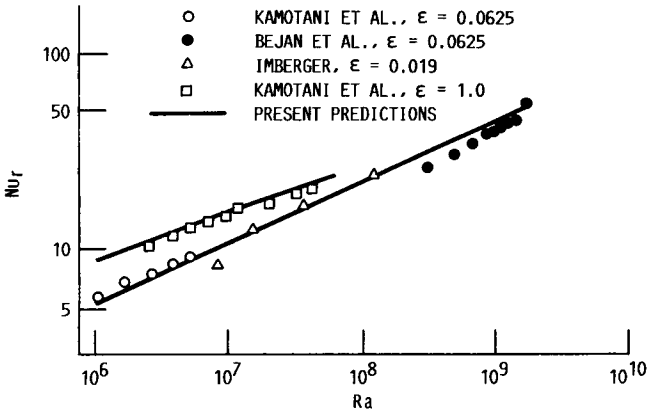

FIGURE 5. - NUSSELT NUMBER IN THE BOUNDARY-LAYER REGIME. (ε, REF. 6.)

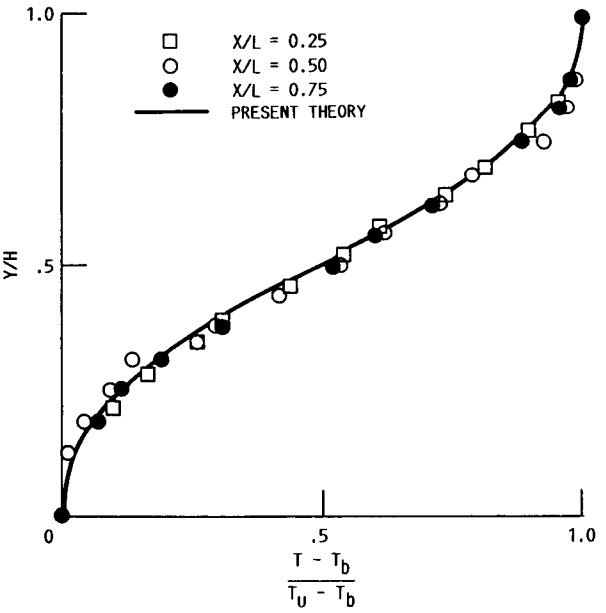

FIGURE 6. - TEMPERATURE DISTRIBUTIONS IN THE CORE REGIONS; ε = 0.0625, Ra = 1.4×10^6, Pr = 6.4. (X/L, REF. 6.)

NASA
National Aeronautics and Space Administration

Report Documentation Page

1. Report No.	2. Government Accession No.	3. Recipient's Catalog No.
NASA TM-100277		

4. Title and Subtitle	5. Report Date
High Rayleigh Number Convection in Rectangular Enclosures With Differentially Heated Vertical Walls and Aspect Ratios Between Zero and Unity	April 1988
	6. Performing Organization Code
7. Author(s)	8. Performing Organization Report No.
Siavash A. Kassemi	E-3838
	10. Work Unit No.
	674-24-05
9. Performing Organization Name and Address	11. Contract or Grant No.
National Aeronautics and Space Administration Lewis Research Center Cleveland, Ohio 44135-3191	
	13. Type of Report and Period Covered
12. Sponsoring Agency Name and Address	Technical Memorandum
National Aeronautics and Space Administration Washington, D.C. 20546-0001	14. Sponsoring Agency Code

15. Supplementary Notes

16. Abstract

High Rayleigh number convection in a rectangular cavity with insulated horizontal surfaces and differentially heated vertical walls has been analyzed for an arbitrary aspect ratio smaller than or equal to unity. Unlike previous analytical studies, a systematic method of solution based on linearization technique and analytical iteration procedure has been developed to obtain approximate closed-form solutions for a wide range of aspect ratios. The predicted velocity and temperature fields are shown to be in excellent agreement with available experimental and numerical data.

17. Key Words (Suggested by Author(s))	18. Distribution Statement
High Rayleigh number Natural convection Confined enclosures Variable aspect ratios	Unclassified - Unlimited Subject Category 34

19. Security Classif. (of this report)	20. Security Classif. (of this page)	21. No of pages	22. Price*
Unclassified	Unclassified	20	A02

NASA FORM 1626 OCT 86

*For sale by the National Technical Information Service, Springfield, Virginia 22161